Chapter 7
Mooring Design for WECs

Lars Bergdahl

7.1 Introduction

7.1.1 General

It would be reasonable that ocean energy devices were designed for the same risk as the platforms in the oil industry. Risk should then be evaluated as a combination of probability of failure and severity of consequences, which means that a larger probability of failure for ocean energy devices would be balanced by the less severe consequences.

The question of some relaxation in safety factors for moorings of WECs has been addressed in the EU Wave Energy Network [1] and at least three times at EWTEC conferences 1995 [2], 2005 [3] and 2013 [4]. Here we will not discuss this but will stick to the present DNV-OS-E301 POSMOOR [5] rules as advised in the Carbon Trust Guidelines [6].

Irregular wave effects are often computed by multiplication of a wave spectrum, for each frequency, with the linear response ratio in that frequency. For instance, using the motion response ratios a response spectrum of the motion will be produced. Thereafter statistical methods can be utilized to assess characteristics of responses in each sea state or in all anticipated sea states during e.g. 50 years.

For large or steep waves and large relative motions non-linear time-domain or non-linear frequency-domain methods must be used, which is out of scope of this chapter.

The goal of the chapter is that the reader shall be able to self-dependently make a first, preliminary analysis of wave-induced horizontal forces, motions and mooring

L. Bergdahl (✉)
Chalmers University of Technology, 41296 Göteborg, Sweden
e-mail: lars.bergdahl@chalmers.se

A. Pecher and J.P. Kofoed (eds.), *Handbook of Ocean Wave Energy*,
Ocean Engineering & Oceanography 7, DOI 10.1007/978-3-319-39889-1_7

tensions for a moored floating WEC. Necessary prerequisites to attain that goal are the understanding of the physical phenomena, awareness of simplifying assumptions and some insight into the available mathematical and numerical tools.

7.1.2 Mooring Design Development Overview

The development of a mooring system will require different steps:

- Defining the environmental conditions
- Perform a quasi-static analysis, requiring to fine-tune the main mooring design parameters in order to fulfil the design rules. The quasi-static design loop for a mooring system is outlined in Fig. 7.1.

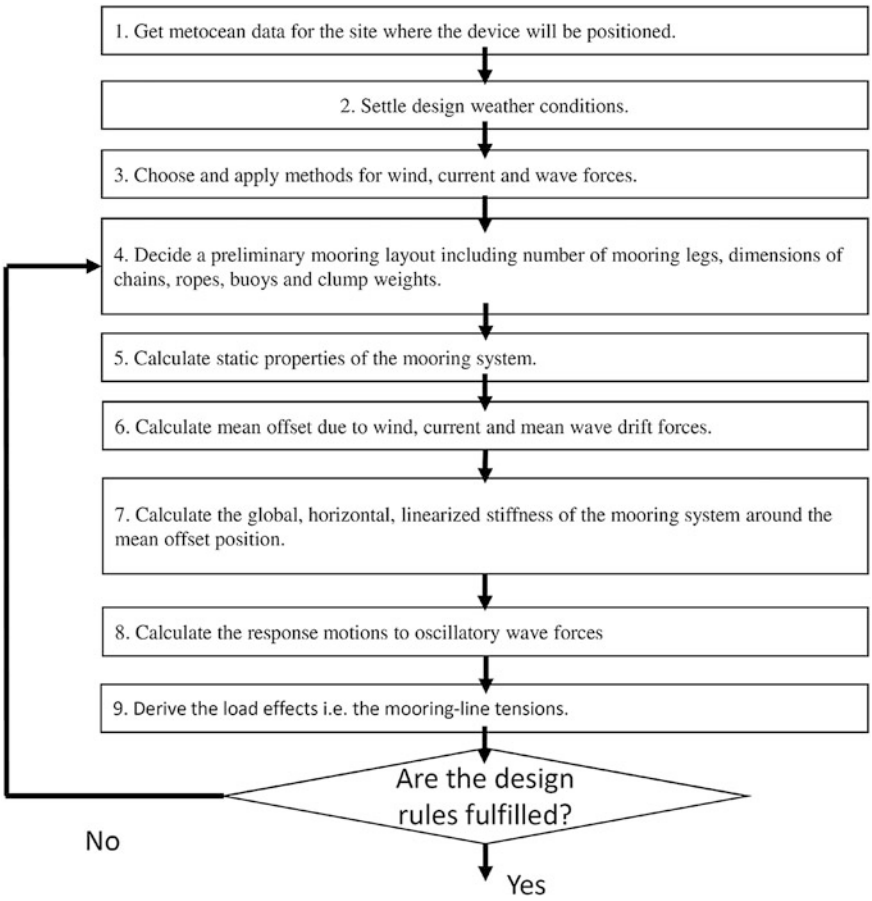

Fig. 7.1 Flow chart of the quasi-static mooring design loop

- Perform model testing to confirm the preliminary quasi-static design. One must then take into account that the moorings may not be correctly modelled due to limitations in water depth or tank width, but some tricks have to be introduced, with springs in the mooring cables compensating for missing cable lengths. Also in some smaller tanks, maybe, the wind and current force cannot be modelled. One then has to preload the mooring system with the calculated mean wind and current force using e.g. a soft horizontal, pre-tensioned spring. Also precaution must be taken concerning the drift force modelling, as small reflexions from the down-wave end of the wave tank may influence the wave drift forces.
  The model testing is based on the assumption that the most important phenomena are governed by potential flow and thus can be modelled using Froude scaling. Drag forces on the whole platform and on the mooring cables are thus not correctly modelled.
- Perform sophisticated dynamic simulations. Such dynamic simulations shall include time varying wind forces, slowly varying wave-drift forces and time series of wave forces. The current could still be considered constant as usually simulations are made for less than three hours duration. Dynamic calculations may first be run in the frequency domain to be able to run many cases. In the end a few critical cases should be run in the time domain.
- Perform prototype tests in the real environment to finally validate the design.

The main design rule is (usually) that the mooring system will be able to ensure the station keeping of the device. In other words, this means that the mooring system will not be overloaded, in terms of tensions in the mooring system and offset of the WEC during the most extreme event it is designed for—usually a 100 year wave.

Comments to the flow chart:

- Weather data may be taken from archived ship born observations, wave buoy data or satellite observations. Wave data can also be "hindcasted" by wave generation models from historical meteorological wind data and also extrapolated by such models to places close to the coast from measurements at off-coast places by a wave generation propagation model like e.g. SWAN [7] or MIKE SW [8]. New measurements may then be started to check the appropriateness of the wave-generation models.
- For the mooring design, usually, combinations of 10-year and 100-year conditions for wind, currents and waves are used, see further Sect. 7.2.4. Before the design conditions are locked it may be wise to confer with the authority or classifying society that will finally verify the mooring design.
- In a quasi-static design mean wind, current and wave drift forces are used for the mean offset and the oscillatory wave force for the dynamic motion response.

7.1.3 Wave-Induced Forces on Structures

One may say that there are two fundamentally different ways to calculate wave-induced forces on structures in the sea. In one method one considers the structure as a whole and assesses the total wave force from empirical or computed coefficients applied on water velocities and accelerations in the undistorted wave motion. This method may be used if the size of the structure is smaller than a quarter of the actual wavelength.

In the other method the pressure distribution around the surface of the structure is computed taking into account the effect on the water motion distorted by the structure itself, and subsequently integrated around the structure. Both these approaches are used for the oscillating wave forces in Sect. 7.3.3.2

In both cases some mathematical model for describing the wave properties is necessary. For instance, by making the simplified assumption that the wave motion can be regarded as potential flow, velocities, accelerations and water motion can be computed in any point under a gravity surface wave by a scalar quantity, the velocity potential.

7.1.4 Motions of a Moored Device in Waves

A moored device in waves will be offset by steady current, wind and wave drift and will oscillate in six degrees of freedom. In very long waves its motion will just follow the sea surface motion with some static reaction from the mooring system, but for shorter waves—near the horizontal and vertical resonances of the body-mooring system—the motion may be strongly amplified and out of phase with the sea surface motion. For still shorter waves the motions will be opposed to the wave motion but less amplified, so when the crest of the wave passes the device the device will be at its lowest position, with obvious consequences for water over-topping the device, or air penetrating under the bottom of the device. For very short waves the wave forces will be completely balanced by the inertia of the device itself and will show negligible motion. Methods for estimating motions of floating objects are described quantitatively in Chap. 10.

7.2 Metocean Conditions

7.2.1 Combinations of Environmental Conditions

The target probabilities of failure and return periods for extreme forces as given in DNV-OS-E301 [5] (POSMOOR) are referred in Tables 7.1 and 7.2. These will be used here as approved, although it may seem reasonable that the safety and

Table 7.1 Target annual probability of failure. For consequence-class definitions see Sect. 7.5.1.2

Limit state	Consequence class	Target annual probability of failure
ULS	1	10^{-4}
ULS	2	10^{-5}

Table 7.2 Return periods for environmental conditions

Return period		
Current	Wind	Waves
10	100	100

reliability requirements for offshore hydrocarbon units exceed those that should be applied to floating ocean wave energy converters.

7.2.2 Design Wave Conditions

According to DNV-OS-E301 [5], sea states with return periods of 100 years shall normally be used. The wave conditions shall include a set of combinations of significant wave height and peak period along the 100-year contour. The joint probability distribution of significant wave height and peak wave periods at the mooring system site is necessary to establish the contour line. If this joint distribution is not available, then the range of combinations may be based on a contour line for the North Atlantic. It is important to perform calculations for several sea states along the 100-year contour line to make sure that the mooring system is properly designed. For instance, moored ship-shaped units are sensitive to slowly varying, low-frequency wave forcing. Therefore, in sea states with shorter peak periods, 6–10 s, the slowly-varying drift force may excite large resonant surge motions, while in a sea state with a long peak period around 20 s the motion is dominated by the wave-frequency motion and the overall damping is larger preventing resonant motion. How to choose sea states along the contour line is indicated in Fig. 7.2. The same values for wind and current shall be applied together with all the sea states chosen along the 100-year contour.

If it is not possible to develop a contour line due to limited environmental data for a location a sensitivity analysis with respect to the peak period for the 100 year sea state shall be carried out. The range of wave steepness criteria defined in DNV-RP-C205 [9] (Paragraph 3.5.5) can then be applied to indicate a suitable range of peak wave periods to be considered in the sensitivity analysis. The JONSWAP spectrum is a reasonable spectrum model for

$$3.6 < T_p/\sqrt{H_s} < 5, \tag{7.1}$$

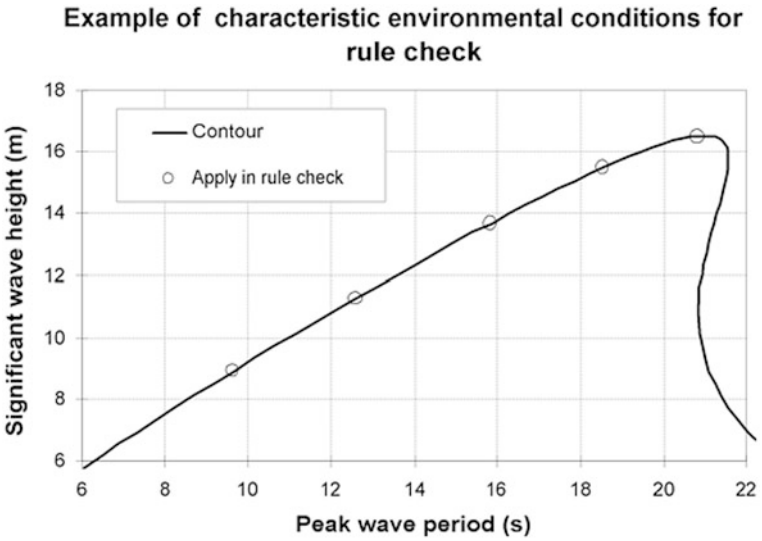

Fig. 7.2 Selections of sea states along a 100-year contour line. (DNV-OS-E301 [5])

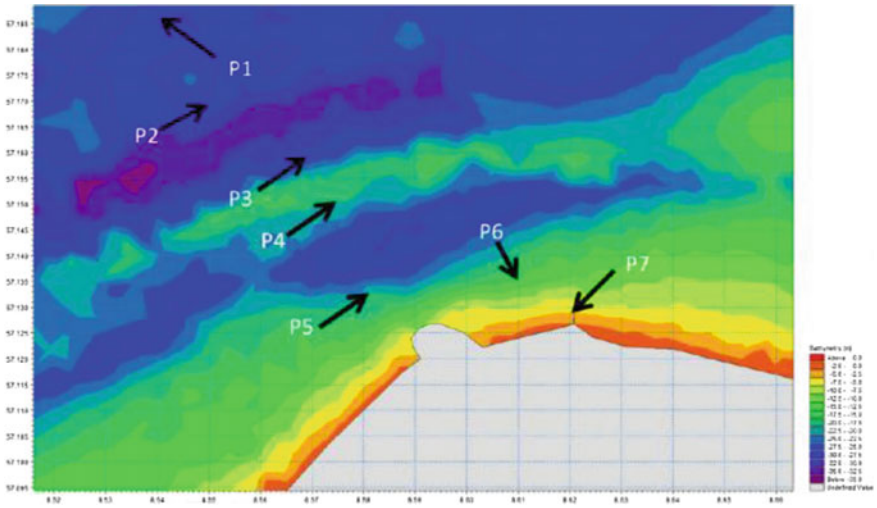

Fig. 7.3 Location of the 7 points with wave data at DanWEC

but should be used with caution outside this range. In the guidance notes in POSMOOR some 100 year contour lines for offshore sites are given. However, they are not very useful in wave energy contexts as wave-energy sites are closer to the coast in shallower areas with milder wave climates. Therefore, it is mostly necessary to use site-specific data, which can be created by using offshore data and

a spectral wave model as SWAN [7] or MIKE 21 SW [8] for transferring the deep water statistics to specific near-shore sites.

7.2.3 Environmental Data at DanWEC

Within the SDWED project, DHI produced data for Hanstholm [10], using MIKE 21 SW [Mean wind speed is taken]. This data will be used for the example mooring design.

The wave conditions for seven points off Hanstholm, Fig. 7.3, have been calculated from the DHI-data by Pecher and Kofoed [11] and are referred in Table 7.3. The individual maximum 100 year wave ($1.86H_s$) may be depth limited as conventionally is approximated by $H_{max} < 0.78h_d$, but at the intended site for the example WEC buoy the water depth is 30 m, why the waves at this site are not depth limited.

Table 7.3 Waves at DanWEC, in front of Hanstholm

		Average Wave conditions				Design wave, Hm0(m)			
	Water depth	Hm0	Tp	T02	Pwave	Return period* (years)			
Location	(m)	(m)	(s)	(s)	(kW/m)	100	50	20	10
P1	29	1.25	6.4	4.2	9.4	9.5	9.1	8.5	8.0
P2	27.5	1.23	6.4	4.2	8.9	9.3	8.9	8.3	7.8
P3	32	1.19	6.3	4.1	8.1	8.8	8.4	7.8	7.4
P4	18.5	1.18	6.4	4.2	8.3	8.9	8.5	7.9	7.4
P5	19	1.09	6.3	4.1	6.8	7.8	7.5	7.1	6.7
P6	14	0.97	6.4	4.0	5.4	6.0	5.9	5.8	5.6
P7	5	0.74	6.6	4.4	2.9	2.7	2.6	2.6	2.5

We also need the design wind, water level and current conditions. Wind and water levels are reported by Sterndorf in a report for WavePlane, and are given below in Tables 7.4 and 7.5.

Table 7.4 Design wind conditions [12]

Probability of exceedance	Wind speed for wind coming from				
	SW	W	NW	N	NE
$V_{wind,3\ h}$ – 1 year (m/s)	21.0	25.0	25.0	19.0	20.0
$V_{wind,3\ h}$ – 10 year (m/s)	24.0	30.0	29.5	23.5	25.0
$V_{wind,3\ h}$ – 100 year (m/s)	28.0	34.0	33.0	28.0	29.0
Probability of wind direction (%)	15.5	18.4	11.8	5.2	8.4

Table 7.5 Design water levels [12]

Probability of exceedance	High water (m)	Low water (m)
3 h 1 year	1.22	1.28
3 h 10 year	1.58	1.52
3 h 100 year	1.96	1.78

Sterndorf gives the wind speed as $V_{wind,\ 3\ h}$, but normally the 10 min mean value is used for mooring design of floating objects.

Sterndorf [12] estimates the current to 3 % of the wind speed, assuming the current to be locally wind generated, yielding 0.68 m/s from SW and 0.58 m/s from NE, while Margheritini [13] cites measured values at 0.5–1.5 m/s coast parallel.

7.2.4 Example Design Conditions

In the sample design calculations below the following values are chosen:

- Mean wind speed is taken from Table 7.4, 100 year return period: $U_{10\ min,10\ m} = 33$ m/s.
- Mean current velocity is set to the maximum measured value according to Margheritini. See text below Table 7.5: 10 year return period: $U_c = 1.5$ m/s
- Waves are taken with guidance from Table 7.3 as representative of Point 3, 4 and 5 to: 100 year return period: $H_s = 8.3$ m.
- A PM-type spectrum as a Bredtscneider or an ISSC-spectrum then gives $T_p = 12.9$ s and $T_{02} = 9.2$ s $< T_z < T_{01} = 9.9$ s. The probable maximum wave height of 1000 waves is then around $H_{max} = H_s 1.86 = 15.4$m.
- Wind, current and waves are acting in the same direction.
- Water depth is taken as $h_d = 30$ m from Pecher et al. [14]

7.3 Estimation of Environmental Forces

7.3.1 Overview and Example Floater Properties

It is demanding to establish the hydrodynamic forces for WECs, because they may undergo very large resonant motion, have very complex shapes composed of articulated connected bodies or involve a net flow of water through the device. This makes it difficult to use conventional potential methods. Probably, most devices need to undergo extensive tank and field testing. However, here we will sketch simplified methods for first estimates of forces useful in the concept stage and for planning tank tests.

In order to design a mooring solution, all environmental forces need be included that can have a significant influence on the motions of the floating body and thereby on the mooring response. The main ones are:

- Wind force
- Sea current force
- Wave forces: Both mean wave drift forces and oscillatory wave forces

The following paragraphs will introduce how these can be estimated for a floating, moored, vertical, truncated, circular cylinder with properties according to Table 7.6.

Table 7.6 Properties of the sample floater

Diameter	(m)	5
Height above mean water surface	(m)	5
Draught	(m)	5
Mass	(tonne)	100
Pitch inertia around mean water surface	(tonne m^2)	1830
Cross coupled inertia ($m_{24} = m_{42} = -m_{15} = -m_{51)}$	(tonne m)	243

7.3.2 Mean Wind and Current Forces

7.3.2.1 Introduction

According to DNV-OS-E301 [5] the wind and current force should be determined by using wind tunnel tests. Wind forces from model basin tests are only applicable for calibration of an analysis model, while the current forces may be estimated from model basin tests or calculations according to recognised theories (DNV-RP-C205 [9], Sect. 7.6.6). In preliminary design also wind forces calculated according to recognised standards may be accepted, such as in DNV-RP-C205 [9], Sect. 7.6.5.

The mean wind and drag force may be calculated using a drag force formulation, with drag coefficients from model tests, or numerical flow analysis. Wind profile according to DNV-RP-C205 [9] and ISO19901-1 shall be applied. Oscillatory wind forces due to wind gusts shall be included:

$$F = CA\frac{1}{2}\rho U^2 \tag{7.2}$$

Here C is traditionally called the shape coefficient for wind force calculations and drag coefficient for current force calculations, A is the cross sectional area projected transverse the flow direction, ρ is the density of the fluid and U is the fluid velocity at the height of the centre of the exposed body. Here we will use the design 10 min mean for the air velocity and the design value of the current, as the response of the horizontal motions and the induced mooring tension are in this time scale.

Values on the coefficient C for different shapes are given in DNV-RP-C205 [9], but can also be found in other standard literature like Faltinsen [15], Sachs [16]. For more complicated superstructures a discussion is found in Haddara and Guedes-Soares [17]. In DNV-RP-C205 there are also guidelines for calculating vibrations or slowly varying wind force due to a wind spectrum.

Below the calculation of the wind and current forces are sketched but more detailed information can be found in DNV-RP-C205.

7.3.2.2 Wind Force on the Sample Floater

Mean wind speed $U_{10\ \mathrm{min},10\ \mathrm{m}} = 33$ m/s.

To use the drag force expression Eq. 7.21 for the wind force we must first estimate the wind speed at the centre of the buoy which is situated 2.5 m above the mean water surface. The wind is given at 10 m height. A wind gradient expression giving the wind speed at 2.5 m from the value at 10 m gives:

$$U(2.5\,\mathrm{m}) = U(10\,\mathrm{m})\left(\frac{2.5\,\mathrm{m}}{10\,\mathrm{m}}\right)^{0.12} = U(10\,\mathrm{m})0.85 = 28.9\frac{\mathrm{m}}{\mathrm{s}} \tag{7.3}$$

In order to estimate the shape coefficient C from graphs and tables in DNV-RP-C205 we must also calculate the Reynolds number:

$$Re = \frac{U_{T,z}D}{v_a} = 9.6\ \times\ 10^6 \tag{7.4}$$

where $D = 5$ m is the diameter and v_a is the kinematic viscosity = 1.45×10^{-5} m^2/s (DNV-RP-C205 [9], APPENDIX F)

Figure 7.25 in DNV-RP-C205 gives C = 1.1 for a relative roughness of 0.01.

The aspect ratio is $2h_b/D = 2$ and gives a reduction factor of $\kappa = 0.8$ for supercritical flow. The height above the water surface of the buoy, h_b, is the same as the diameter, D, and it is considered as mirrored in the water surface to calculate the aspect ratio, which is defined as the length over width ratio.

Thus the wind force is (Air density $\rho_a = 1.226$ kg/m^3 at 15 °C)

$$F_a = \kappa C D h_b \frac{1}{2}\rho_a U_{T,z}^2 = 10.5\ \mathrm{kN} \tag{7.5}$$

7.3.2.3 Current Force on the Sample Floater

The current speed is assumed to have no vertical gradient close to the free water surface and the mean current speed $U_c = 1.5$ m/s. In order to estimate the drag coefficient C from graphs and tables in DNV-RP-C205 we must estimate the

Reynolds number. Diameter D = 5 m, and the kinematic viscosity $v_w = 1.19 \times 10^{-6}$ m^2/s, thus the Reynolds number is $Re = \frac{U_c D}{v_w} = 6.3 \times 10^6$.

Again Fig. 7.25 in the DNV-RP-C205 gives again C = 1.1 for a relative roughness of 0.01

The aspect ratio is $2D_b/D = 2$ and gives a reduction factor of $\kappa = 0.8$ for supercritical flow. The draught below the water surface of the buoy, D_b, is the same as the diameter, D, and again it is considered as mirrored in the water surface to calculate the aspect ratio.

Thus the current force is (Sea water density ρ = 1025.9 kg/m^3 at 15 °C)

$$F_c = \kappa C D D_b \frac{1}{2} \rho U_c^2 = 24.5 \text{ kN} \tag{7.6}$$

7.3.3 Wave Forces

7.3.3.1 Mean Wave Drift Force

Mean Wave Drift Force in Regular Waves, Simplified Approach

Basically there are two alternative approaches to estimate the wave drift force. The first approach involves integrating the pressure over the instantaneously wetted surface of the body. This will, for a body in a regular wave, give a force composed by a mean force, a force at the same frequency as the incident wave (the usual first-order wave force, which will be discussed in the next section) and a force at the double frequency. For the slowly varying drift forces only the mean force is of interest. The second approach involves utilising the momentum conservation and will be used here. We will approximate it in 2D for a terminator type body subjected to a plane, unidirectional wave motion with the incident wave amplitude a.

Through a vertical the time mean of the incident momentum per unit width of structure is

$$I_0 = \frac{\rho g a^2}{4} \tag{7.7}$$

If this wave is blocked by a vertical wall, a wave with the same amplitude, $r = a$, will be reflected in the opposite direction and the momentum acting on the wall, or mean drift force will become

$$F_d = I_{in} - I_{out} = \frac{\rho g}{4}(a^2 + r^2) = 2I_o = \frac{\rho g a^2}{2} \tag{7.8}$$

This is the largest possible mean wave drift force on a floating body per unit width of structure. For a floating 2D body, however, not all the energy will be reflected and the body will be set in motion and radiate energy up-wave and down-wave. If we denote the amplitude of the combined reflected and back-radiated wave by r and the amplitude of the combined transmitted and down-wave radiated wave by t, then a momentum approach will give

$$F_d = \frac{\rho g}{4}(a^2 + r^2 - t^2) \tag{7.9}$$

This was set up by Longuet-Higgins [18]. Maruo [19] stated that if there are no losses in the flow, the sum of the powers in the r wave and the t wave must equal the power in the incident wave, i.e. $(a^2 = r^2 + t^2)$ and consequently

$$F_d = \frac{\rho g}{2} r^2 \tag{7.10}$$

For successful WECs this equation is not valid, as then $a^2 \gg r^2 + t^2$ and thus for complete wave absorption in the limit $F_d = \rho g a^2/4$. For a device in standby again Eq. 7.9 is valid.

For real devices with limited transverse extension the above equations can be seen as upper bounds as the wave is scattered around the object and waves are radiated by the object in the horizontal plane.

Mean Wave Drift Force in Irregular Waves

A very simple approach on the conservative side is based on the assumption that the object reflects all waves in the opposite direction to the incoming waves for all component waves, with the amplitude, a_i. In e.g. a PM-spectrum with H_s = 8.3 m the drift force would be:

$$F_d = \frac{1}{2}\rho g \sum\nolimits_i \frac{1}{2} a_i^2 D = \frac{\rho g H_s^2}{32} D = 108 \text{ kN} \tag{7.11}$$

The above equation presumes that all components would be reflected without any scatter. However an object with a diameter less than one quarter of a wavelength diffracts or reflects negligible energy. In our case this wave length is 4 D = 20 m corresponding to the wave period 3 s and frequency 0.28 Hz. Plotting a PM-spectrum with H_s = 8.3 m and drawing the line for f = 0.28 Hz gives the following picture that indicates that the wave drift force would be negligible, as almost the entire spectrum is below this frequency (Fig. 7.4).

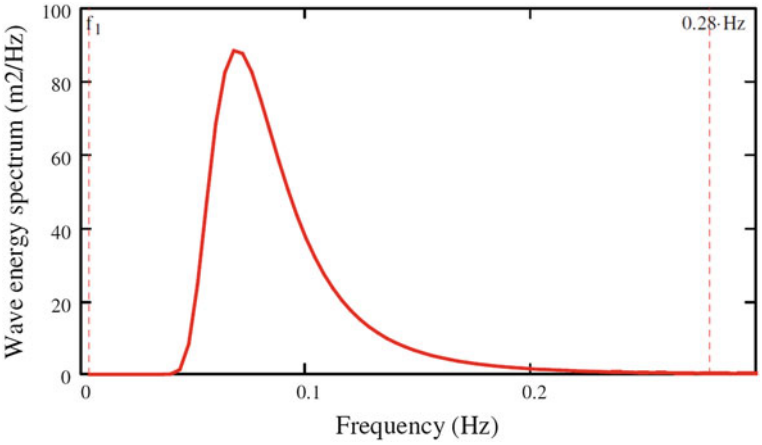

Fig. 7.4 The design wave energy spectrum, PM-spectrum with H_s = 8.3 m. The wave period 0.28 Hz corresponding to a deep-water wave length of 4 D is marked in the figure

To check that the drift force really is small in the survival design storm with H_s = 8.3 m, we have calculated the drift force coefficient for the floating buoy with WADAM [20] and integrated the total drift force in that sea state, see Fig. 7.5. Using WADAM's definition of the drift-force coefficient, the drift force can be written

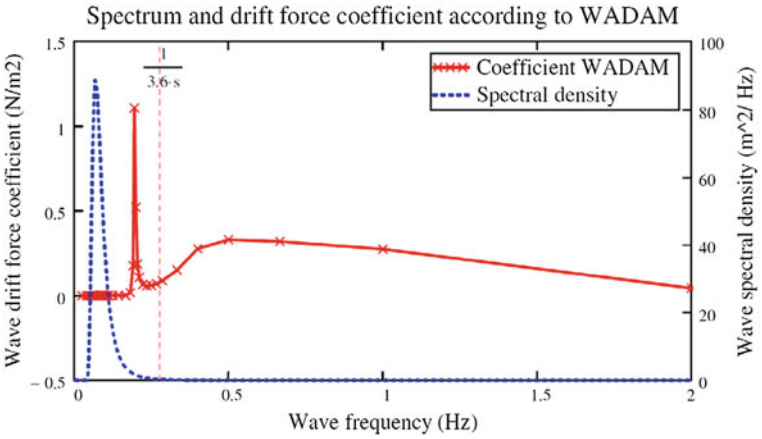

Fig. 7.5 The drift force coefficient as a function of wave frequency as calculated by WADAM [9]. Note the effect of the vertical resonant motion at 0.2 Hz

$$F_d = 2\rho g D \sum_i C_{d_i} \frac{1}{2} a_i^2 \tag{7.12}$$

The resultant drift force was found to be F_d = 2.5 kN, which in this case is 25 % of the estimated wind force and 10 % of the current force and can thus—as a first

approximation—be neglected in the design storm. In operational sea states with shorter waves and lower wave heights the drift force may be of the same magnitude as the wind and current forces, but all three forces are smaller. The drift force of 2.5 kN will be used in the example below.

7.3.3.2 First-Order Wave Forces

Overview

The first approach to calculating wave forces on bodies in water was founded on the assumption that the body does not affect the water motion and pressure distribution in the incident wave. Nowadays one would normally use diffraction theory, taking into account the scatter of the incident wave caused by the body.

In Fig. 7.6 we can note different flow regimes as function of $\pi D/\lambda$ and H/D. In the present case $\pi D/\lambda = \pi D/(g\ T_p^2/2\pi) \approx 0.06$ and $H_{max}/D \approx 3$, which set us in the inertia and drag regime. For such bodies with a characteristic diameter of less than 1/4 to 1/5 of a wave length the effect on the wave is small, and the wave force can, as an approximation, be set to the sum of an inertia term and a drag term. The

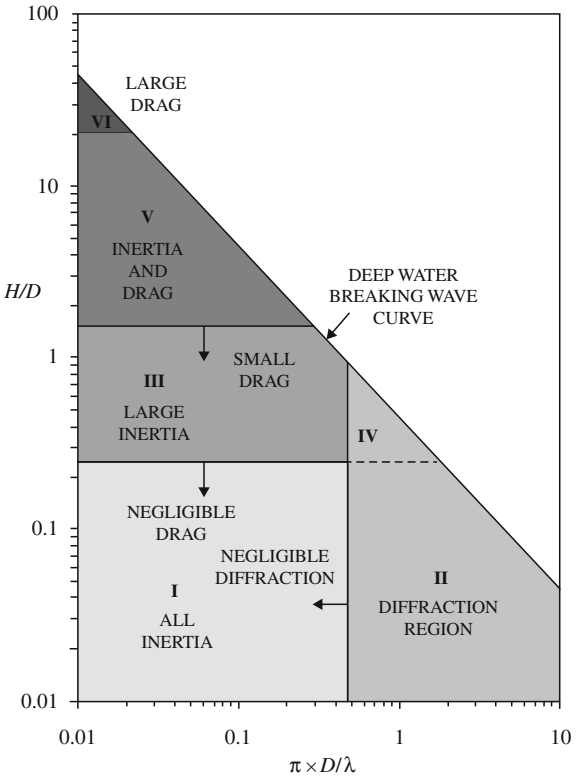

Fig. 7.6 Different wave force regimes (Chakrabarti 1987, cited by DNV). D = characteristic dimension, H = sinusoidal wave height, λ = wave length. Adapted from DNV-RP-C205 [9]

inertia term is the product of the displaced mass, added mass included, and the undisturbed relative water acceleration in the centre of displacement. The drag term depends on the relative velocity between water and body. In surge this so called Morison formulation is:

$$F = \rho V \frac{du}{dt} - m\ddot{x} + C_m \rho V \left(\frac{du}{dt} - \ddot{x} \right) + \frac{1}{2} C_D \rho A |u - \dot{x}|(u - \dot{x}) \tag{7.13}$$

Where:

- F is the reaction force from e.g. a mooring system (Unmoored body $F = 0$)
- ρ is the density of water
- V the displaced volume
- u and $\frac{du}{dt}$ the undisturbed horizontal water velocity and acceleration in the centre of the body
- m the mass of the body
- x the horizontal position of the body
- $\ddot{x}$ and $\dot{x}$ the acceleration and velocity of the body
- C_m an added mass coefficient (Can be taken from standard values in e.g. DNV-RP-C205 [9])
- C_D a drag coefficient (Can be chosen from recommendations in e.g. DNV-RP-C205)
- A the cross-sectional area in the direction perpendicular to the relative velocity

So far we have not defined any properties of the mooring system, but for the time being we can assume that the body is fixed to select the coefficients C_m and C_D, again using DNV-RP-C205 [9]. One should then take into account the variation of C_D and C_m as functions of the Reynolds number, the Keulegan-Carpenter number and the relative roughness.

$$\begin{aligned} &\text{Reynolds number} : Re = u_{max} D/v \\ &\text{Keulegan-Carpenter number} : \mathrm{KC} = u_{max} T/D \\ &\text{Relative roughness} : k/D \end{aligned}$$

where:

- D = diameter = 5 m
- T = wave period = T_p = 12.9 s
- k = roughness height = 0.005 m
- u_{max} = maximum water velocity in a period $\pi H_{max}/T_p$ = 3.8 m/s (assuming circular water motion in deep water) and
- $\nu_w = 1.19 \times 10^{-6}$ m^2/s = fluid kinematic viscosity.

For the buoy $Re = 8 \times 10^6$, KC = 10 and k/D = 10^{-3}. For coefficients of slender structures DNV-RP-C205 still refers to Sarpkaya and Isacson [21] but the problem is that their graphs and experience are limited to Re < 15×10^5, see also

Chakrabarti [22]. Anyway, these graphs and also equations in DNV-RP-C205, Sect. 7.6.7, point to $C_D = 1$ and $C_m = 1$ for circular cylinders. As for the steady flow the drag coefficient may be reduced to 0.8 due to the aspect ratio. In Appendix D, RP-C205, Table D-2 there is also an indication that C_m could be reduced to around 0.8 due to the aspect ratio $L/D = 2$

Wave Forces on "Small" Bodies D < L/4

Wave Forces in a Regular Wave (Small Body)

Applying the Morison equation above for the fixed body, it reduces to

$$F = \rho V(1 + C_m)\frac{du}{dt} + \frac{1}{2}C_D \rho A|u|u \tag{7.14}$$

This force, as a function of time for the wave amplitude $a = H_{max}/2$ and period $T = T_p$, is drawn in the figure below together with the horizontal water acceleration. One can note that the evolution in time is affected by the drag, but that the maximum value is almost unaffected, and can approximately be calculated as the mass (inertia) force amplitude:

$$F_M = \rho V(1 + C_m)\left.\frac{du_a}{dt}\right|_{max} = 0.44 \text{ MN} \tag{7.15}$$

The mass force amplitudes $F_M = \pm 0.44$ MN are drawn as horizontal lines in the graph. The drag-force maximum is $F_D = 0.3$ MN but is 90 degrees out of phase with the water acceleration and in phase with the water velocity (Fig. 7.7).

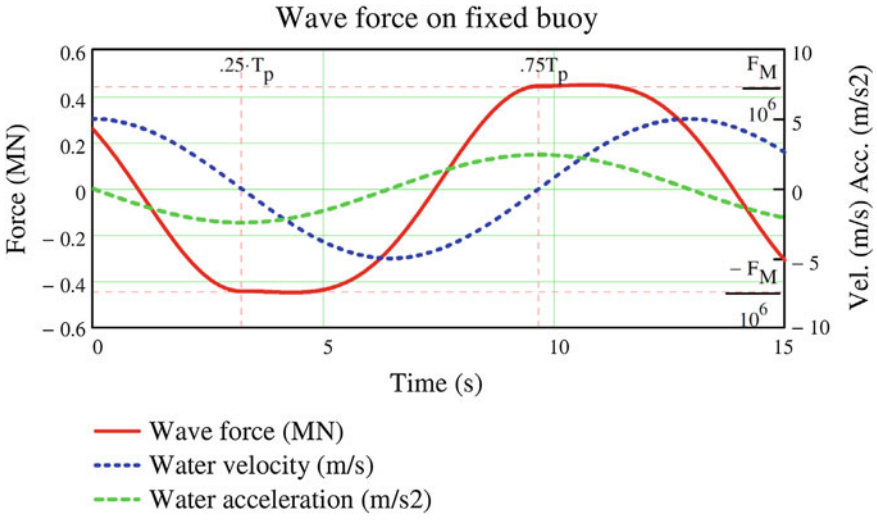

Fig. 7.7 The Morison force as a function of time for wave amplitude a = $H_{max}/2$ and period T_p = 12.9 s. The water acceleration is drawn for comparison

We can note that the wave force amplitude is one order of magnitude larger than the mean force from wind, current and wave drift. However, for a floating moored body the wave force would be carried by the inertia of the body and not by the mooring or positioning system as we do not want to counteract the wave-induced motion only prevent the buoy from drifting off its position.

Wave Forces in Irregular Waves (Small Body)

If we neglect the drag term in the wave force equation above, we can calculate the wave force spectrum, $S_F(f)$, directly by multiplication of the wave spectrum, $S_{PM}(f)$ by the square of the wave force ratio, $f_w(f)$. The problem is that for $f > 0.28$ Hz the diffraction would be important and the small body assumption is not valid. The force amplitude divided by the wave amplitude or force amplitude ratio (also known as RAO) would become

$$\begin{aligned} f_w(f) = \frac{F}{a} = \frac{\rho V}{a}(1+C_m)\frac{du}{dt}_{max} = \rho V(1+C_m)gk\frac{\cosh(k(z+h))}{\cosh(kh)} \quad & f < 0.28 \text{ Hz and} \\ f_w(f) = 0 \quad & f > 0.28 \text{ Hz.} \end{aligned} \tag{7.16}$$

where $k = 2\pi/L$ is the wave number. In deep water $k = \mathrm{g}/\omega^2 = g/(2\pi)^2$.

The wave force spectrum could then be calculated as

$$S_F(f) = (f_w(f))^2 S_{PM}(f) \tag{7.17}$$

These functions are drawn in Fig. 7.8

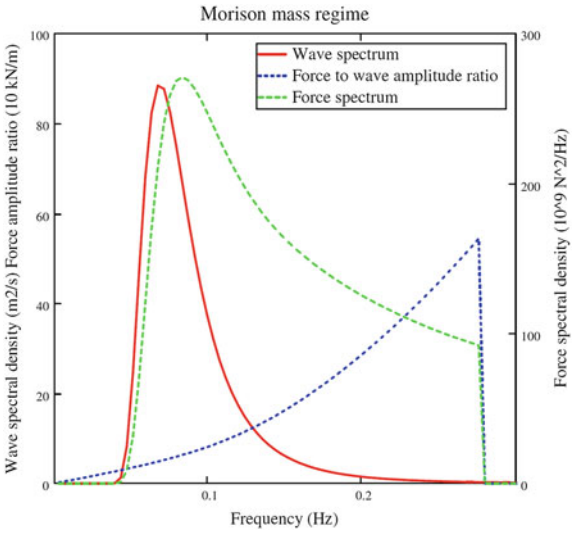

Fig. 7.8 Wave energy spectrum, $S_{PM}(f)$, force amplitude ratio, $f_w(f)$, and force spectrum, $S_F(f)$. Morison approach

The significant force amplitude is then

$$F_{Msamp} = 2\sqrt{m_{0F}} = 2\sqrt{\int_{0\ \mathrm{Hz}}^{0.28\ \mathrm{Hz}} S_F(f)df} = 0.38\ \mathrm{MN} \tag{18}$$

And the maximum force in 3 h would be $F_{Mmax} = 1.86\ F_{M\,samp} = 0.71$ MN.

This is similar to calculating the significant wave height and relation between H_{max} and H_s, but here it is the Rayleigh distribution for the for the amplitudes, that is why there is $2\sqrt{m0}$ and not $4\sqrt{m0}$ in Eq. 7.20.

Wave Forces on "Large" Bodies

Overview

To extend the force calculation to shorter waves or relatively larger bodies we are forced to use diffraction theory, which is more demanding and, yet, does not take drag (viscous) forces into account. On the other hand radiation damping caused by waves generated by the motion of the body in or close to the free surface is included, which lacks in the Morison approach. For the diffraction problem of the vertical circular buoy there are analytical series solutions available e.g. in Yeung [23] and Johansson [24] (Figs. 7.9 and 7.10). Here we will illustrate it by using results from Johansson. Bodies with general form can be calculated in panel diffraction programs like WAMIT [20].

In Figs. 7.9, 7.10 and 7.11, graphs with added mass, radiation damping and wave force amplitude ratio as functions of frequency are displayed. The wave force amplitude ratio will be used immediately for comparison of wave forces on the fixed body. The added mass and radiation damping will be used later for calculating wave motion and slowly varying wave drift motion of the moored buoy (Fig. 7.11).

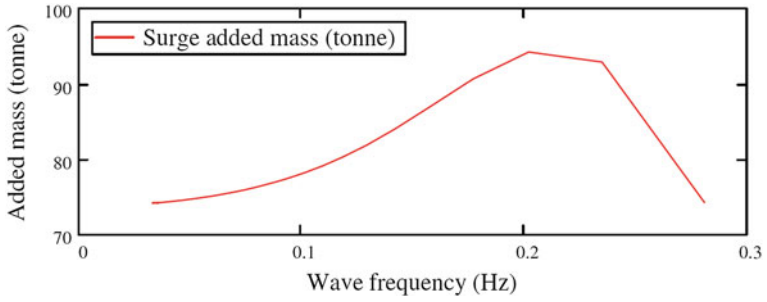

Fig. 7.9 Surge added mass, A_{11}, as a function of wave frequency

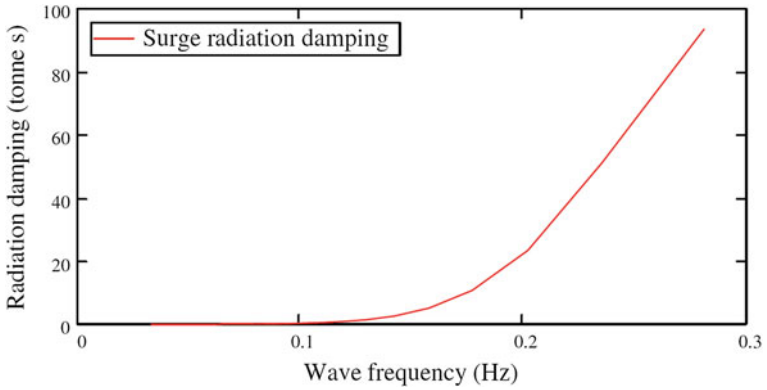

Fig. 7.10 Surge radiation damping, B_{11}, as a function of wave frequency

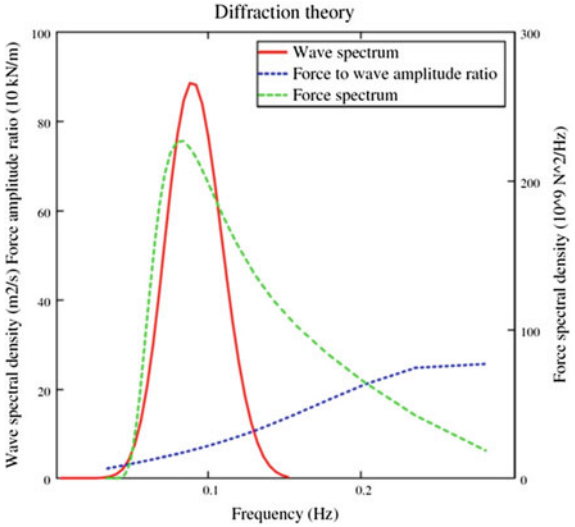

Fig. 7.11 Wave energy spectrum, $S_{PM}(f)$, force amplitude ratio, $f_{dw}(f)$, and force spectrum, $S_{dF}(f)$. Diffraction results from Johansson [24]

Wave Forces in Irregular Waves (Large Body)

The wave force spectrum can now be calculated as before but with diffraction results instead of approximate coefficients

$$S_{dF}(f) = (f_{dw}(f))^2 S_{PM}(f) \tag{7.19}$$

The significant force amplitude is now estimated as

$$F_{dsamp} = 2\sqrt{m_{0dF}} = 2\sqrt{\sum_i S_{dF}(f_i)\Delta f_i} = 0.30 \text{ MN} \tag{7.20}$$

And the maximum force in 3 h would be $F_{dmax} = 1.86\ F_{dsamp} = 0.55$ MN.

The 23 % reduction of the force is due to the lower force amplitude ratio according to the diffraction theory compared to the Morison model. Note especially that the diffraction force ratio has a maximum around 0.3 Hz in this case and actually will decrease for higher frequencies while the Morison counterpart grows to infinity (Fig. 7.12). This is more realistic than the overestimated force in the Morison mass approach for irregular waves in Sect. 7.3.3.2.2.2

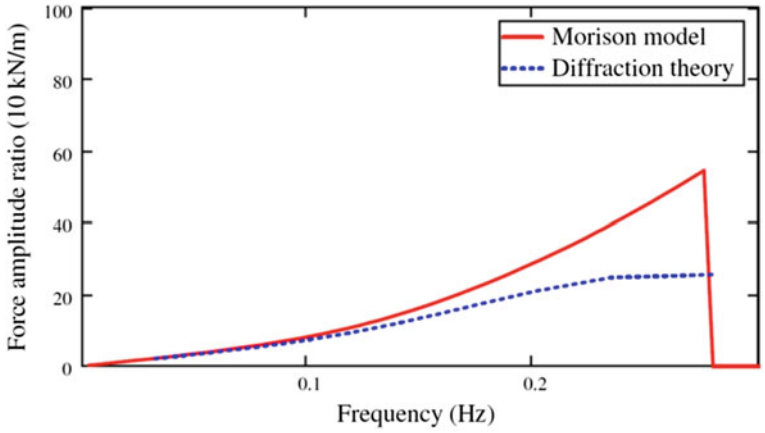

Fig. 7.12 Force amplitude ratio according to the Morison approach and diffraction theory

In the quasi-static mooring design approach, we need estimate the motion of the moored object in regular design waves or in an irregular sea state. To get the mooring force we must know the statics of the mooring system.

7.3.4 Summary of Environmental Forces on Buoy

In Table 7.7 there is a summary of results from the gradually more sophisticated calculations. First one can note that—in this case—the simplest wave-drift estimate gives 40 times as large value as the one founded on diffraction theory. This is important in relation to the wind and current force. The Morison wave force for a regular sinusoidal wave is very dependent on the assumed wave period, while the Morison approach for irregular waves gives some better significance, however some 20 % overestimation.

Shaded values will be used in the design as they are considered as most realistic.

Table 7.7 Key results from force estimates on the floating buoy

Mean loads		Force (kN)	Wave force	Force (MN)	
Wind	33 m/s	10.5	Morison Regul. $H_{max}/2 = 7.7$ m	0.44	Amplitude
Current	1.5 m/s	24.5	Morison mass regime Irregul. $H_s = 8.2$ m	0.38	Significant
Wavedrift $H_s = 8.2$ m	Simple	108		0.71	Most prob. maximum
	Diffraction	2.5	Diffraction Irregul. $H_s = 8.2$ m	0.30	Significant
Total mean	Simple	143		0.55	Most prob. maximum
	Diffraction	37.8			

Shaded values will be used in the design

7.4 Mooring System Static Properties

7.4.1 Example

For illustrative purposes a mooring configurations will be used as presented by Pecher et al. [14]: a three-leg Catenary Anchor Leg Mooring system, CALM, see Fig. 7.13.

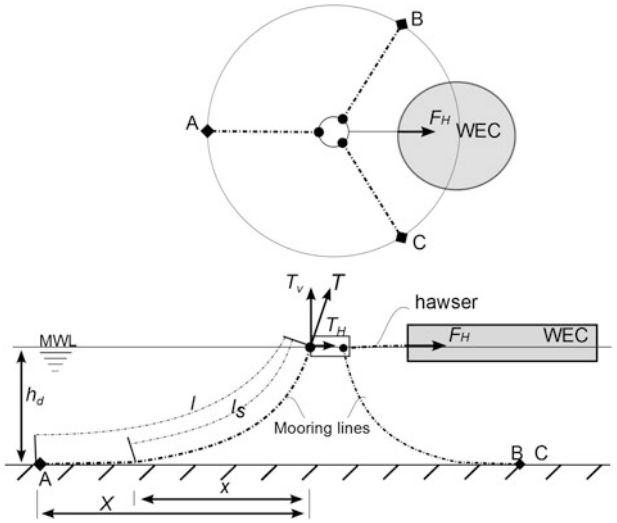

Fig. 7.13 Sketch of a three-leg Catenary Anchor Leg Mooring (CALM). [14]

The CALM system is composed of three chain-mooring legs directly fastened to the example buoy. This is different to the example by Pecher et al. [14] who have assumed that the mooring legs are connected to a mooring buoy, which in turn is coupled by a hawser to a wave-energy device. The legs have equal properties listed in Table 7.8. The lengths of the mooring lines should be chosen such that they will just lift all the way to the anchor when loaded to their breaking load.

Table 7.8 Example properties of the CALM system

Three-leg system 120 deg	Chain Steel grade Q3	Notation
Water depth	30 m	h_d
Horizontal pretension	20 kN	H_p
Unstretched length	509 m	s
Breaking load	2014 kN	T_B
Diameter	50.4 mm	
Mass per unit unstretched length	53.65 kg/m	q_o
Weight in sea water per unit unstretched length	457 N/m	γ_r
Axial stiffness	228 MN	$K = EA$

7.4.2 Catenary Equations

Here we will use the equations for an elastic catenary expressed in the unstretched cable coordinate from its lowest point, or from the touch-down point at the sea bottom as in Fig. 7.13, to a material point, s_o [25].

The horizontal stretched span or the horizontal distance, $x_{o1}(s_o)$, from the touch-down point, $s_o = 0$, is

$$x_{o1}(s_o) = a \operatorname{arcsinh}\left(\frac{s_o}{a}\right) + \frac{\gamma_r a}{K} s_o, \tag{7.21}$$

and the vertical span is

$$x_{o2}(s_o) = \sqrt{a^2 + s_o^2} + \frac{\gamma_r}{2K} s_o^2 - a, \tag{7.22}$$

where $a = H/\gamma_r$ i.e. the horizontal force divided by the un-stretched weight per unit length in water. Solving for the lifted cable length, s_o, for $x_{o2}(s_o) = h_d$ = the water depth, we can now express the total distance to the anchor $X(H)$ including the part of chain resting on the sea floor as a function of the horizontal force, H.

$$X(H) = x_{o1}(s_o(H)) + (s - s_o(H))\left(1 + \frac{H}{K}\right) \tag{7.23}$$

or inversely the horizontal force $H(X)$ as a function of the stretched span X, Fig. 7.14

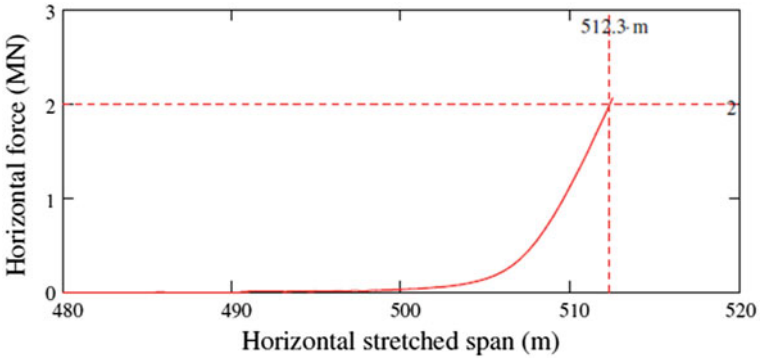

Fig. 7.14 The horizontal force as function of the horizontal, stretched span

In the intended system we have assumed a pretension of H_p = 20 kN at zero excursion. This corresponds to a horizontal span of $X(H_p)$ = 498.36 m. Finally we can add the reaction of the three legs to get the total horizontal mooring force as a function of the excursion, $x = X(H) - X(H_p)$, in the x-direction in parallel to the upwind leg.

$$F_{tot}(x) = H(x) - 2\cos(60^\circ)H\left(-\frac{x}{\cos(60^\circ)}\right) \tag{7.24}$$

In the example we can see that almost all the horizontal force is carried by the cable in the up-wave direction as soon as the excursion exceeds 4 m.

Last we need calculate the horizontal stiffness, $S(x)$, of the mooring system, that is, the slope of the blue function displayed in Figs. 7.15 and 7.16.

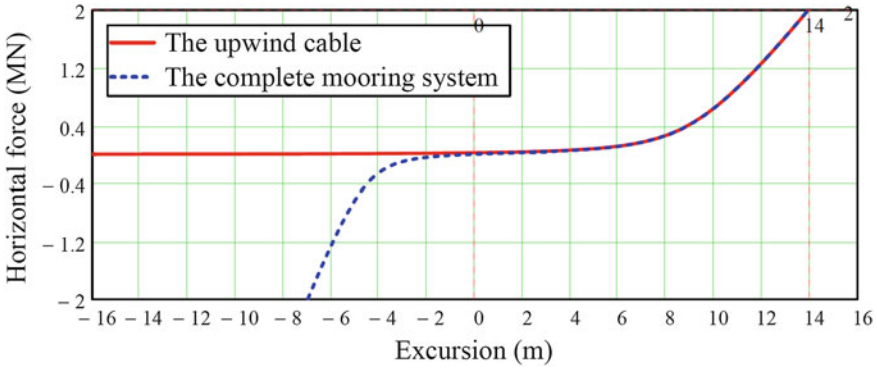

Fig. 7.15 Horizontal force as a function of the excursion of the buoy. The up-wave cable takes most of the force

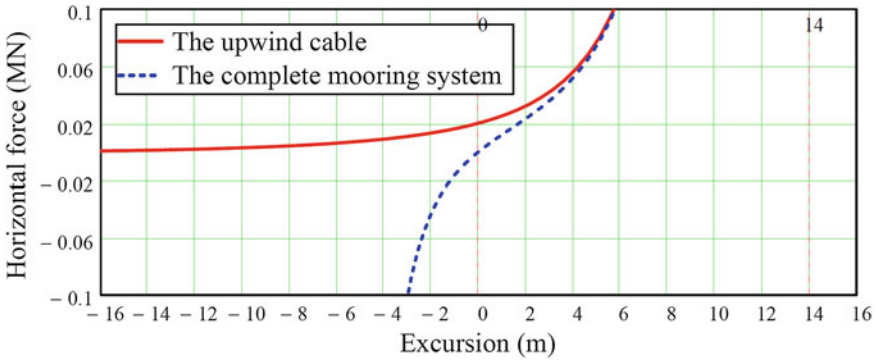

Fig. 7.16 Horizontal force as a function of the excursion of the buoy. Different range of vertical axis compared to Fig. 7.15

It is interesting to note that the stiffness for negative excursion is larger than for positive excursion, which is caused by having two interacting legs in this direction (Fig. 7.17).

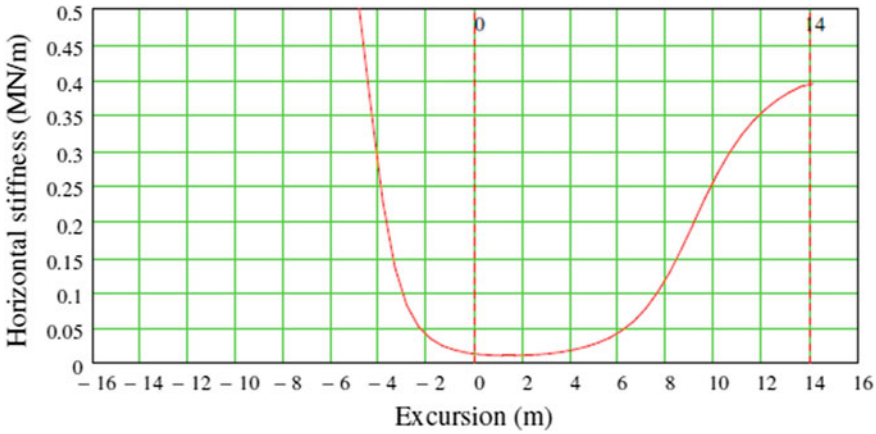

Fig. 7.17 The horizontal stiffness of the mooring system as a function of the excursion

7.4.3 Mean Excursion

The horizontal motion should be calculated around the mean offset (excursion). Therefore the offset due to the mean forces is calculated using the methods described above. We also need the mooring stiffness around the mean offset. The result is given in Table 7.9.

Table 7.9 Summary of offset and mooring stiffness due to the mean environmental forces

Mean force	Force	Mean offset	Tangential Stiffness
	(kN)	(m)	(kN/m)
Wind + current + WADAM wave drift	10.5 + 24.5 + 2.5 = 37.5	2.6	12

7.5 Alternative Design Procedures

7.5.1 Quasi-Static Design

7.5.1.1 Quasi-Static Design Procedure

The most used method for designing mooring systems is still a variant of the quasi-static design procedure, described for instance by Selmer [26] (see Fig. 7.18).

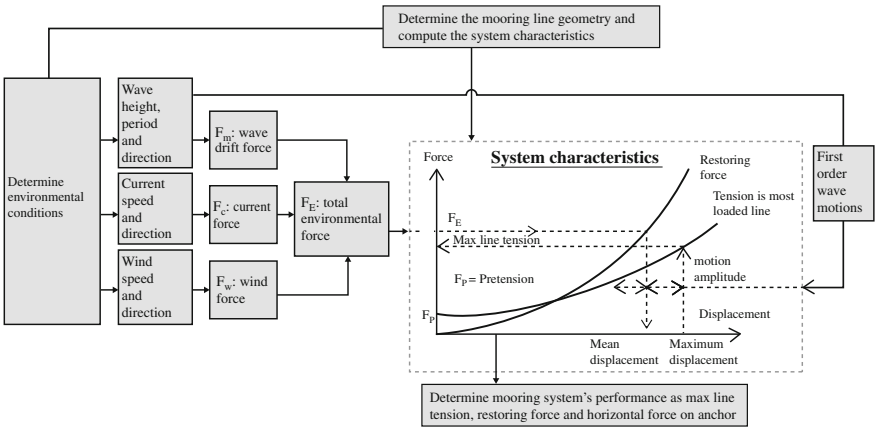

Fig. 7.18 Quasi-static analysis. Adapted from [26]

1. Wind, current and wave-drift forces are considered constant and acting in the same direction.
2. The horizontal reaction force as a function of offset is calculated for the mooring system, and from this the offset and cable tensions due to the constant forces.
3. The motion of the freely floating platform is calculated for the design sea state.
4. The maximum horizontal offset due to the wave induced motions is added to the constant offset, and the corresponding (static) cable tensions are obtained from the static functions calculated in step 2.
5. The tension force in the most loaded cable is compared with the allowed force for operational or survival conditions.

In modern quasi-static procedures, first, constant forces from mean wind, mean current and mean wave drift are assumed acting co-linearly on the moored floating object, as is stated in DNV-OS-E301 POSMOOR [5] of Det Norske Veritas (DNV). This gives a mean horizontal offset in the force direction. The equation of motion for the moored floating object—including the stiffness of the mooring system—is then solved so that possible resonance effects are taken into account. In the original approach, described above, the wave-induced motion for the freely floating platform was used, assuming that the mooring system did not have any effect on the motion. This is not recommended nowadays, but gives small errors for large floating platforms reasonably deep water with soft mooring systems adding resonance only outside the wave-frequency range.

Sometimes, time-domain simulations with non-linear static mooring reaction are performed, but wave frequency and low-frequency motion responses may alternatively be calculated separately in the frequency domain and added. In the latter case, a horizontal, linearized mooring stiffness is used. In DNV-OS-E301 the larger of the below combined horizontal offsets is thereafter used for calculation of quasi static line tension

$$\begin{aligned} X_{C1} &= X_{mean} + X_{LF-max} + X_{WF-sig} \\ X_{C2} &= X_{mean} + X_{LF-sig} + X_{WF-max} \end{aligned} \tag{7.25}$$

where X_{C1} and X_{C2} are the characteristic offsets to be considered, X_{mean} is the offset caused by the mean environmental forces and, $X_{LF\text{-}max}$ and $X_{LF\text{-}sig}$ are, respectively, the maximum and significant offset caused by the low-frequency forces and $X_{WF\text{-}max}$ and $X_{WF\text{-}sig}$ the maximum and significant offset caused by the wave-frequency forces. The low- and wave-frequency motions shall be calculated in the mean offset position using the linearized mooring stiffness in the mean position. By the index max is meant the most probable maximum amplitude motion in three hours. By the index sig is meant the significant amplitude motion in three hours. If the standard deviation of motion is σ, then the significant offset is 2σ, and the most probable maximum offset is $\sqrt{0.5 \ln N} 2\sigma$ in N oscillations which means 3.72σ in 1000 waves (T_z = 11 s) and maybe 3σ in the slowly varying oscillations (N = 100, T_z = 110 s).

The tension caused by the greater of the two extreme offsets according to Eq. 7.25 is subsequently used to calculate the design tension in the most loaded mooring leg. For a conventional catenary system this would be in a windward mooring leg at the attachment point to the floating device.

7.5.1.2 Safety Factors

In DNV-OS-E301 two consequence classes are introduced in the ULS and ALS, defined as:

- *Class 1*, where mooring system failure is unlikely to lead to unacceptable consequences such as loss of life, collision with an adjacent platform, uncontrolled outflow of oil or gas, capsize or sinking.
- *Class 2*, where mooring system failure may well lead to unacceptable consequences of these types.

The calculated tension $T_{QS}(X_C)$ should be multiplied by a partial safety factor $\gamma = 1.7$ for Consequence Class 1 and quasi-static design from Table 7.10, and the product should be less than 0.95 times the minimum breaking strength, S_{mbs}, when statistics of the breaking strength of the component are not available:

$$\gamma T_{QS} < 0.95 S_{mbs} \tag{7.26}$$

or expressed by a utilization factor, u, which should be less than 1:

$$u = \frac{\gamma T_{QS}}{0.95 S_{mbs}} < 1 \tag{7.27}$$

Table 7.10 Partial safety factors for ULS, DNV-OS-E301 [5]

Consequence class	Type of analysis	Partial safety factor for mean tension	Partial safety factor for dynamic tension
1	Dynamic	1.10	1.50
2	Dynamic	1.40	2.10
1	Quasi-static	1.70	
2	Quasi-static	2.50	

A requirement for a slack catenary system with drag-embedment anchors is also that the mooring cables must not lift from the bottom all the way to the anchor.

Table 7.10 is quoted from DNV and contains safety factors for dynamic design, which are not used here but included for completeness.

First Design Loop

As described in Sect. 7.5.1.1 the calculated tension $T_{QS}(X_C)$ should be multiplied by a partial safety factor $\gamma = 1.7$ for Consequence Class 1 and the product should be less than 0.95 times the minimum breaking strength, S_{mbs}.

For the present example results of the design calculation are given in Table 7.11, see Sect. 7.6.8. As can be seen the calculation with the horizontal mooring stiffness $S = 12$ kN/m does not fulfil the strength requirements above, and thus we need to do a second design round with a modified mooring system.

Table 7.11 Comparison between required tension and calculated tension

Design offset (m)		Lifted chain length (m) at X_{C2}	T_{QS} (MN)	γT_{QS} (MN)	$0.95S_{mbs}$ (MN)	u
X_{C1}	X_{C2}					
7.8	12.3	424	1.38	2.35	1.9	1.23

Studless chain Q3 diameter 50.4 mm. Offset stiffness 12 kN/m

Second Design Loop

Solving Inequality 27 for the minimum breaking strength with T_{QS} = 1.38 MN gives a required minimum breaking strength to 2.5 MN. This corresponds e.g. to a stud chain Grade 3 diameter 58 mm [27] with S_{mbs} = 2.6 MN, a mass of 77 kg/m [28] and a stiffness of 296 MN [5]. A second design loop was performed with this chain and diffraction methods including linearized damping, see Tables 7.12 and 7.13. The usage factor is now 1.03 which is almost permissible. Adding 31 m to the cable gives a slightly more elastic (softer) mooring which fulfils $\gamma T_{QS} = < 0.95\, S_{mbs}$ and the usage factor u = 0.99 < 1.

Table 7.12 Design offsets for quasi-static design

Mean offset	Stiffness	Wave frequency amplitude		Low frequency amplitude		Design offset		Lifted chain length at X_{C2}
(m)	(kN/m)	(m)		(m)		(m)		(m)
		Sign.	Max.	Sign.	Max.	X_{C1}	X_{C2}	
3.4	13.3	5.3	9.9	0	0	8.7	13.3	370

Diffraction results with equivalent drag damping for stud chain Grade 3 diameter 58 mm

Table 7.13 Comparison between required tension and calculated tension for stud chain Grade 3 diameter 58 mm, 509 m and 540 m long chains

Stiffness	Design offset		Lifted chain length at X_{C2}	T_{QS}	γT_{QS}	$0.95S_{mbs}$	U
(kN/m)	(m)		(m)	(MN)	(MN)	(MN)	
	X_{C1}	X_{C2}					
509 m long cable							
13.3	8.7	13.3	370	1.50	2.55	2.47	1.03
540 m long cable							
13.2	8.7	13.3	362	1.44	2.45	2.47	0.99

7.5.2 *Dynamic Design*

7.5.2.1 Dynamic Design Using Uncoupled Mooring Cable Dynamics

In the simplest dynamic design, the time domain motion of the attachment points of the mooring cables is fed into some cable dynamics program to produce dynamic forces in the cables. This is especially vital for reproducing the maximum tensions in the cables. In Fig. 7.19 as an example, time traces of measured cable tension, tension simulated in the cable dynamics program MODEX [29] and tension calculated from the static elastic catenary are plotted, the latter two using the measured fairlead motion as input. One can observe that the dynamically calculated tension is fairly close to the measured tension, while the quasistatic tension is much too small. A similar observation was made in analyses for the WaveBob [30]. This was often referred to as Dynamic Design around 1990. In DNV-OS-E301 [5] this is the standard procedure for the mooring line response analysis. Programs containing this approach are, e.g., MIMOSA [31], ORCAFLEX [32], ZENMOOR [33] and SIMO [34]. SIMO, in combination with the cable dynamics program RIFLEX [20], has been used by Parmeggiano et al. [35]. for the Wave Dragon.

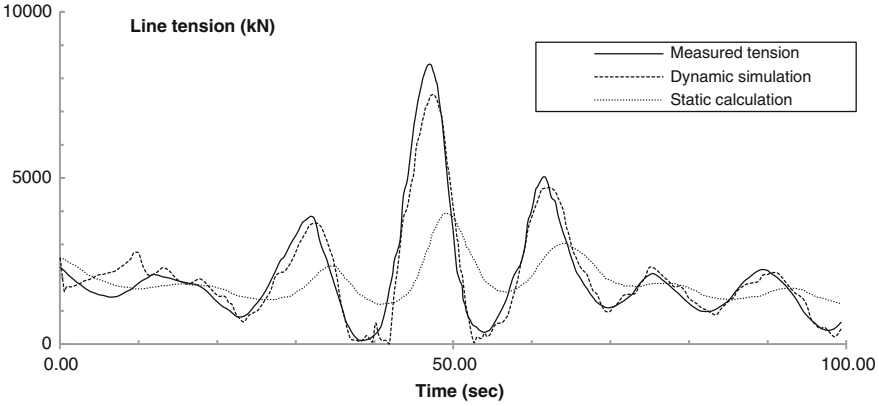

Fig. 7.19 Course of cable tension around the time for maximum tension in a model test of GVA 5000P (Troll C). [29]

7.5.2.2 Coupled Analysis

In modern computer packages for mooring design "fully" coupled mooring analysis is often included, for example, DeepC [36], CASH [20], Orcaflex [32]. In such analyses, the floater characteristics are first calculated in a diffraction program and then time-domain simulations are run using convolution techniques with "full" dynamic reaction from all mooring cables and risers. Time series of cable and riser tensions, floater motions, air gap, etc. are output. Typically, around 10–20

realisations for each specified combination of environmental conditions (Sea state, wind speed and current velocity) are run and statistics of platform motions and cable and riser forces are subsequently evaluated. Still, the wave-induced motion is based on small-amplitude wave theory and small-amplitude body motion and viscous effects may only be included by drag formulations. This may be less inaccurate for large platforms, with moderate motions compared to their size, than for WECs. Fully coupled analysis is often used as a final check in the design, for example, for Thunder Horse [37], with a displacement of 130,000 tonnes. A fully coupled analysis of multiple wave energy converters in a park configuration is described by Gao and Moan [38], and the PELAMIS team used Orcaflex for coupled analysis of the moorings [39].

7.5.2.3 Coupled Analyses with Potential or CFD Simulations

The next natural step would be to exchange the diffraction calculation of the floating body for a non-linear potential simulation with free surface [40] or CFD RANS simulation also containing viscosity. Efforts in the latter direction for WECs are made by, for example, Palm et al. [41], and by Yu and Li [42]. Processor times are still large, but are gradually becoming more affordable.

7.5.3 Response-Based Analysis

Recently, it has become common to check the final design that was based on some specified N-year environmental combination. This is done within the framework of a "response-based analysis" using long time series of real and synthesised environmental data. For instance, such an analysis was made for the Jack & St Malo semisubmersible for Chevron [43], with 145,000 tonnes displacement, even larger than the Thunder Horse. A representative, but synthesised, 424 year period of data for every hour (3.8 million time stamps) was used as a basis. From this basis, around 380000 statistically independent "worst" events were selected. Running dynamic simulations on all these 380000 events is impractical, so these events were first screened in quasi-static analyses and around 1900 events were selected with extreme responses above specified levels. Again, the selected 1900 events were simulated by dynamic runs in the program SIMO using a somewhat simplified input for current drag and viscous effects. Of the 1900 events, around 220 met higher extreme response levels. Finally, these 220 events were simulated in SIMO with an updated current drag model calibrated against model tests for each sea state. In a statistical analysis, the N-year response was calculated and compared to the responses of the N-year environmental design combinations. In this case, the responses to the N-year design conditions were found to be worse or equal to the simulated N-year responses for both 100 and 1000 year return periods [44].

It may be anticipated that in the future response-based analysis could be used for a last check of the design of ocean energy converters.

7.6 Response Motion of the Moored Structure

7.6.1 Equation of Motion

The forces on a floating body can be constant as the mean force in Sect. 7.4.3, transient i.e. of short duration or harmonic. Irregular or random forces from e.g. sea waves can to a first, linear approximation be treated as a superposition of harmonic forces, an approach that will be used here. The responses are fundamentally different for the three types of forces. The present buoy—mooring system will be treated as a single-degree-of-freedom (SDoF) system as illustrated in Fig. 7.20.

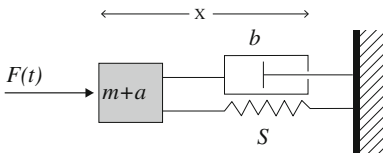

Fig. 7.20 A mechanical system with one degree of freedom, mass, m, added mass, a, damping coefficient, b, and spring stiffness, S

The equation of motion for this system can be written

$$(m+a)\ddot{x} + b\dot{x} + Sx = F(t) \tag{7.28}$$

For bodies in water the mass inertia is increased by an "added mass", a, or hydrodynamic mass. In our case this is represented by the C_m coefficient. This is a result of the fact that to accelerate the body it is also necessary to accelerate the water surrounding the body. For submerged bodies close to the water surface the added mass can be negative, but for deeply submerged bodies it is always positive. For bodies vibrating in or close to the water surface the damping, b, is caused by the radiation of waves from the motion of the buoy and also by linearized viscous damping through the drag force. The coefficients a and b are functions of the motion frequency, or wave frequency in waves, see e.g. Figs. 7.9 and 7.10 for the sample buoy. S is the mooring stiffness and $F(t)$ is the driving force.

General mechanics of vibration can be found in some fundamental textbooks e.g. books by Craig [45], Roberts and Spanos [46] or Thompson [47].

7.6.2 Free Vibration of a Floating Buoy in Surge

Before the discussion of response to different types of forcing we will repeat a little about the free vibrations of the one-degree-of-freedom system. The equation of motion for a buoy in surge can be written

$$(m+a)\ddot{x} + b\dot{x} + Sx = 0 \tag{7.29}$$

which follows directly from Eq. 7.28 setting $F(t) = 0$.

Assuming a solution of the form

$$x = Ce^{\kappa t} \tag{7.30}$$

we get the characteristic equation

$$\kappa^2 + 2\xi\omega_N\kappa + \omega_N^2 = 0 \tag{7.31}$$

where

- $\omega_N = \sqrt{S/(m+a)}$ is the "natural" angular frequency, that is, the undamped angular frequency
- $\xi = b/\left(2\sqrt{S(m+a)}\right)$ is the damping factor.

$$\text{The roots of } \kappa^2 + 2\xi\omega_N\kappa + \omega_N^2 = 0 \tag{7.32}$$

are

$$\kappa_{1,2} = -\xi\omega_N \pm \omega_N\sqrt{\xi^2 - 1}. \tag{7.33}$$

These roots are complex, zero or real depending on the value of ξ. The damping factor can thus be used to distinguish between three cases: underdamped ($0 < \xi < 1$), critically damped ($\xi = 1$) and overdamped ($\xi > 1$). See Fig. 7.21 for the motion of a body released from the position $x(0) = 1$ m at $t = 0$ s. The underdamped case displays an attenuating oscillation, while the other cases display motions monotonously approaching the equilibrium position. A moored floating buoy in surge would normally display underdamped characteristics with a damping factor of the order of 10^{-3}. Note that an unmoored buoy, $S = 0$ exhibits no surge resonance. The damping factor is often called the damping ratio, as it is equal to the ratio between the current damping coefficient, b, and the critical damping coefficient, $2\sqrt{c(m+a)}$.

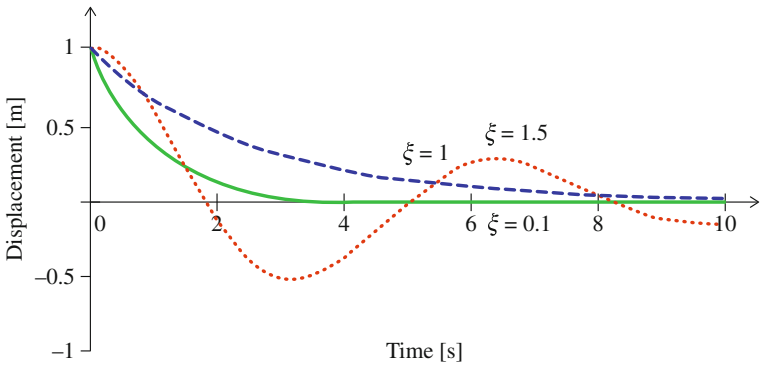

Fig. 7.21 Response of a damped SDOF system with various damping ratios

The natural frequency and damping factor for the moored buoy at the mean offset are listed in Table 7.14. As the peak period is $T_p = 12.9$ s and the zero-crossing period is $T_{02} = 9.2$ s $< T_z < T_{02} = 9.9$ s in the design spectrum, there is a risk for horizontal resonant motion.

Table 7.14 Natural frequencies and damping factors for the moored buoy at the mean offsets

Mean offset (m)	Stiffness (kN/m)	Natural period (s)	Damping factor
2.6	12.0	24.4	0.09×10^{-3}

7.6.3 Response to Harmonic Forces

A harmonic force

$$F(t) = F_o \cos(\omega t) \tag{7.34}$$

as from regular waves for instance gives a response of the same harmonic type:

$$x(t) = \hat{x}\ \cos(\omega t - \varepsilon). \tag{7.35}$$

The motion $x(t)$ is the stationary response to the harmonic force and is the particular solution to Eq. 7.28 with the right hand side $F(t)$ given by Eq. 7.34

F_o is the force amplitude

$\omega = 2\pi/T$ the angular frequency $\quad T$ the time period

$\hat{x}$ the amplitude of the displacement and $\quad \varepsilon$ the phase lag between the force and displacement (Fig. 7.22).

We can solve

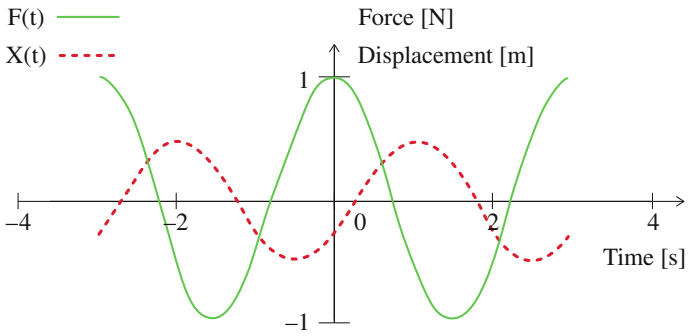

Fig. 7.22 The exciting harmonic force $F(t)$ and the stationary Response, $x(t)$, for a linear system

$$(m+a)\,\ddot{x} + b\dot{x} + Sx = F(t) \tag{7.28}$$

for the given harmonic force,

$$F(t) = F_o \cos(\omega t) \tag{7.34}$$

simply by substituting the particular solution Eq. 7.35 into it. The last equation gives the surge velocity and acceleration of the buoy:

$$\begin{aligned} x &= \hat{x}\cos(\omega t - \varepsilon) \\ \dot{x} &= -\omega\hat{x}\sin(\omega t - \varepsilon) \\ \ddot{x} &= -\omega^2\hat{x}\cos(\omega t - \varepsilon) \end{aligned}$$

The substitution gives

$$(S - (m+a)\omega^2)\hat{x}\cos(\omega t - \varepsilon) - b\omega\hat{x}\sin(\omega t - \varepsilon) = F_o\cos(\omega t) \tag{7.36}$$

Using the trigonometric expressions for sine and cosine of angle differences then after some manipulation yields the amplitude $\hat{x}$, which by definition is positive.

$$\hat{x} = \frac{F_o}{\sqrt{\left\{(S - (m+a)\omega^2)^2 + b^2\omega^2\right\}}} \tag{7.37}$$

We can solve for the phase angle, ε, also, but this is not of interest in the present context. In Fig. 7.23 a graph is drawn of the horizontal response amplitude ratio, i.e. the surge motion amplitude divided by the wave force amplitude, as a function of frequency. The frequencies corresponding to the peak and mean periods are marked to point out the sensitivity to the forcing frequency.

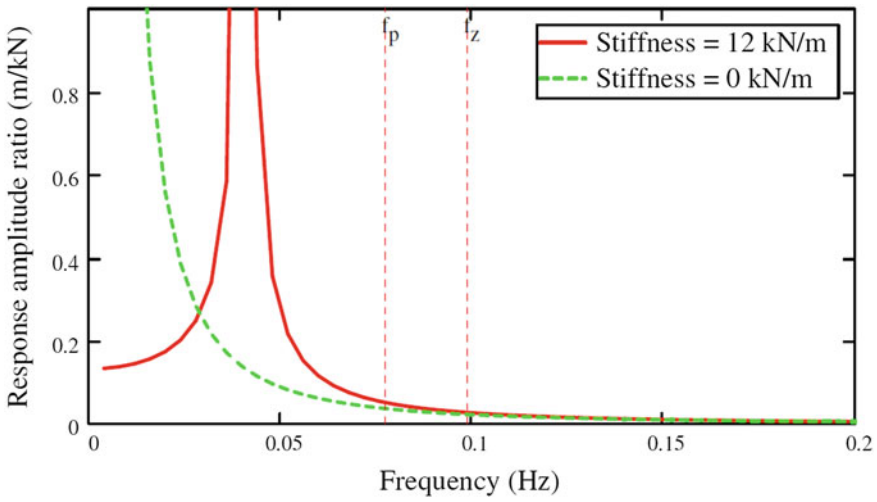

Fig. 7.23 The horizontal response amplitude ratio, surge motion amplitude divided by the wave force amplitude, as a function of frequency. The frequencies corresponding to the peak and mean periods of the wave spectrum are marked to point out possible effects of the forcing frequency

In Table 7.15 the amplitude of the excursion around the mean offset is listed for a regular waves with the periods T_p and $T_z = T_{01}$ with the force amplitude $F_o = F_{Msamp} = 0.38$ MN, i.e. the value of significant force amplitude. In the case of a fixed structure the maximum wave would produce the largest force on the structure. However, for the motion of a moored structure Eq. 7.36 gives the asymptotic motion amplitude after several regular force cycles, while the maximum wave just is a transient incident. It may therefore be more appropriate to use the significant wave height, combined with the peak or mean period. Because the system is very sensitive to resonance, we need include drag damping in a time-domain model or at least linearized drag damping to get near realistic results. Note that the motion amplitude of an unmoored buoy exhibits a smaller motion amplitude due to the absence of resonance.

Table 7.15 Motion amplitude due to a regular Morison wave force, $F_0 = F_{Msamp} = 0.38$ MN

Stiffness (kN/m)	Amplitude at f_p (m)	Amplitude at f_z (m)	Mean offset (m)	Combined excursion (m)	
				at f_p	at f_z
12	12.3	6.5	2.6	14.9	9.1
Unmoored	8.8	5.4		8.8	5.4

7.6.4 Response Motion in Irregular Waves

7.6.4.1 Morison Mass Approach

Using the wave force spectrum based on the Morison mass force approach

$$S_F(f) = (f_w(f))^2 S_{PM}(f), \tag{7.38}$$

we can calculate the surge motion response spectrum as [22]

$$S_x(f) = \frac{S_F(f)}{(S-(m+a)\omega^2)^2 + b^2\omega^2} = \frac{(f_w(f))^2 S_{PM}(f)}{(S-(m+a)\omega^2)^2 + b^2\omega^2} \tag{7.39}$$

Then the significant motion amplitude can be estimated as

$$x_{1s} = 2\sqrt{m_{0dF}} = 2\sqrt{\sum_i S_x(f_i)\Delta f_i} \tag{7.40}$$

The result of this calculation is shown in Fig. 7.24 and in Table 7.16 below on the lines marked "none" under linearized drag damping. Without consideration of the drag damping the motion becomes unrealistically large as the large horizontal drag damping is not taken into account. It is much larger than the surge radiation damping.

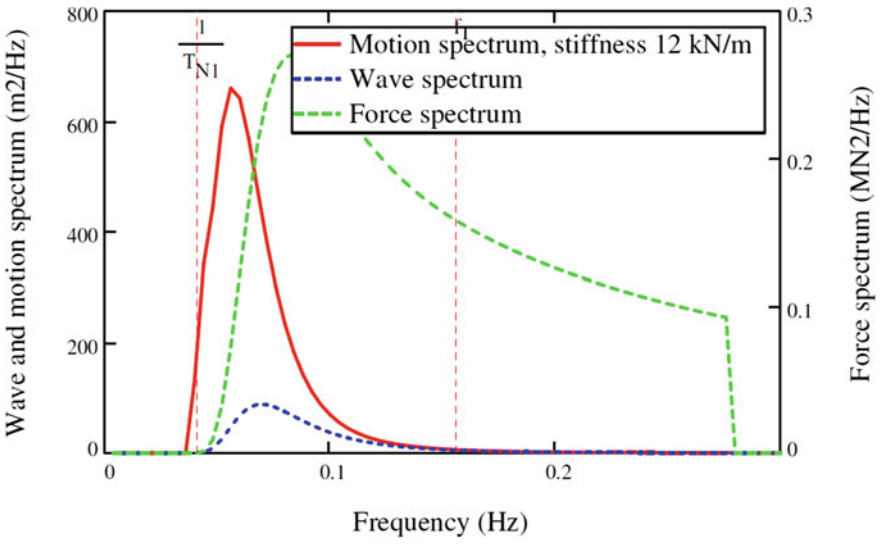

Fig. 7.24 Motion spectra, wave spectrum and force spectrum as functions of frequency. Morison mass approach. No viscous damping. The natural motion period is also marked as $1/T_{N1}$

Table 7.16 Significant linear response in an irregular wave, PM-spectrum, H_s = 8.3 m

Mean offset (m)		Stiffness (kN/m)	Linearized drag damping	Significant amplitude (m)
2.6	Morison	12	None	7.3
2.6	Diffraction	12	None	9.5
2.6	Diffraction	12	Included	5.2

7.6.4.2 Diffraction Force Approach

Using the wave force spectrum based on diffraction forces we can similarly form a diffraction-based surge spectrum:

$$S_{dF}(f) = (f_{dw}(f))^2 S_{PM}(f) \tag{7.41}$$

we can calculate the surge motion response spectrum as [22]

$$S_{dx}(f) = \frac{S_{dF}(f)}{(S-(m+a)\omega^2)^2 + b^2\omega^2} = \frac{(f_{dw}(f))^2 S_{PM}(f)}{(S-(m+a)\omega^2)^2 + b^2\omega^2} \tag{7.42}$$

Then the significant motion amplitude can be estimated as

$$x_{d1s} = 2\sqrt{m_{0dF}} = 2\sqrt{\sum_i S_x(f_i)\Delta f_i} \tag{7.43}$$

The result of this calculation is shown in Fig. 7.25 and in Table 7.16 on the lines marked diffraction and "none" under linearized drag damping. Without consideration of the drag damping the motion becomes also here unrealistically large.

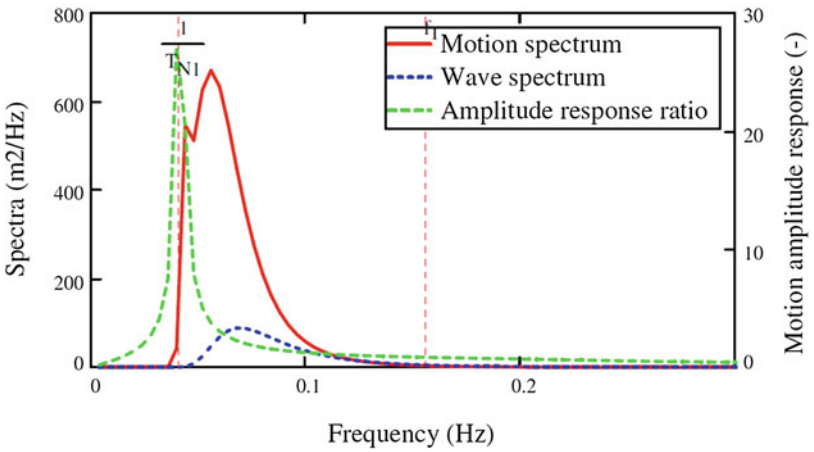

Fig. 7.25 Motion spectrum and wave spectrum as functions of frequency for the stiffness 12 kN/m. The natural frequency $1/T_{N1}$ is marked. Diffraction approach. No viscous damping

7.6.5 Equivalent Linearized Drag Damping

Neglecting the coupling between surge and pitch we can symbolically write the drag damping surge force as

$$F_{D1} = K|u - \dot{x}_1|(u - \dot{x}_1), \tag{7.44}$$

where K can be set to $(1/2)\rho C_D D h_b$ and u is the undisturbed horizontal velocity of the water in the surge direction and $\dot{x}_1$ the surge velocity of the buoy.

When the non-linear surge damping is important usually $u \ll \dot{x}_1$ and then we can set

$$F_{D1} = K|\dot{x}_1|(\dot{x}_1), \tag{7.45}$$

which is simpler but still non-linear.

To assess an equivalent linear coefficient we can compare the dissipated energy over a time, say 3 h, with an equivalent linear expression and the surge velocity

$$x_1(t) = \sum\nolimits_i (\sqrt{2S_x(f_i)\Delta f_i}\cos(\omega_i t + \varepsilon_i)) \tag{7.46}$$

Then the dissipated energy can be calculated in two ways

$$\int_0^T K|\dot{x}_1|(\dot{x}_1)^2 dt = \int_0^T B_{e11}(\dot{x}_1)^2 dt, \tag{7.47}$$

$$\therefore B_{e11} = K\frac{\int_0^T |\dot{x}_1|(\dot{x}_1)^2 dt}{\int_0^T (\dot{x}_1)^2 dt} \tag{7.48}$$

That is, the equivalent damping coefficient, B_{e11}, depends on the modulus of the surge motion, $|\dot{x}_1|$. The result of this calculation is shown in Table 7.16 on the line marked "included" under linearized drag damping. It should be warned that the specific set of wave components and phase angles used in the numerical realisation affects the equivalent damping and significant amplitudes. In our case we got around 8 m significant amplitude for one realisation and around 5 m for another one. However, we may now be able to accommodate the motion. In Fig. 7.26, there is a comparison between surge response spectra with and without linearized drag damping.

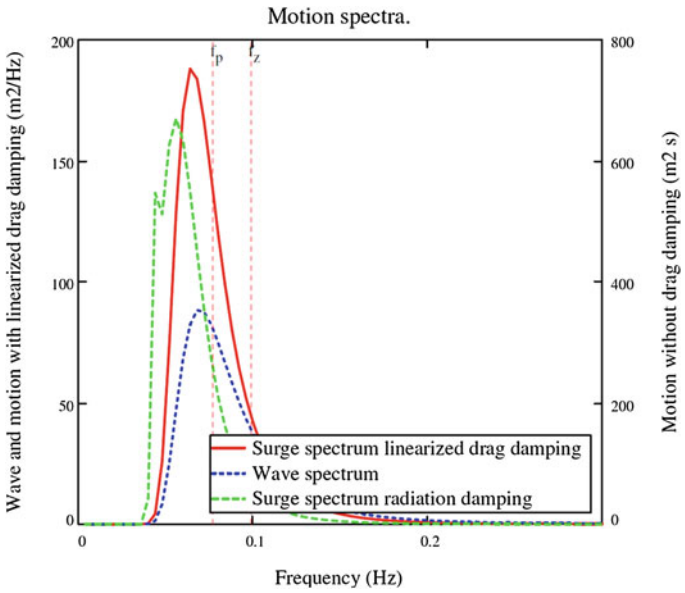

Fig. 7.26 Wave spectrum and surge spectra with and without equivalent linearized damping for the stiffness 12 kN/m. Note the different vertical scales

7.6.6 Second-Order Slowly Varying Motion

In cases where the second-order slowly varying wave force hits the resonance of the moored system, second order slowly varying motion may become large and induce motions of the same order of magnitude as the first-order wave induced motions.

The low-frequency excitation force can be expressed in the frequency-domain by a spectrum [48].

$$S_{LF}(\mu) = 8\int_0^\infty S(\omega)S(\omega+\mu)C_d\left(\omega+\frac{\mu}{2}\right)\mathrm{d}\omega \tag{7.49}$$

Here $S(\omega)$ is the wave spectrum and $C_d(\omega)$ is the wave drift force coefficient. The equation is invoking the Newman [49] approximation and cannot be used if the resonance period is within the wave spectrum periods. Then the full non-linear expression should be used, see e.g. [15]. In the present case this is not the case and, anyway, in such cases the motion is dominated by the first-order wave-excited motion.

A sample calculation for this case gives negligible second order slowly varying motion—surge amplitude in the order of mm—compared to the first-order motion. The first and second order motions can be comparable in lower sea states. The reason for negligible second order slowly varying motion is that the resonance period is off the peak of the drift force spectrum and that the drift force coefficient is

small. On the other hand, we should maybe have used the full non-linear expression. However, experience gives that the second-order motions for small objects in high sea states display little second-order motions. See Fig. 7.27, where a range of horizontal resonance angular frequencies from 0.3 to 0.6 rad/s for realistic offsets is marked.

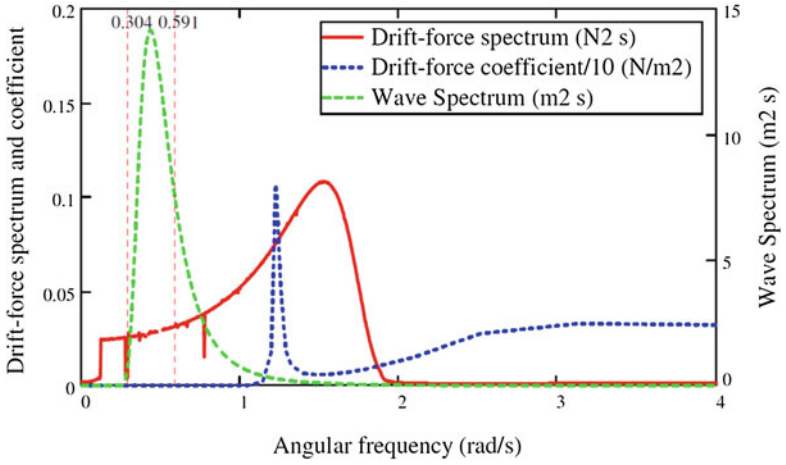

Fig. 7.27 Drift-force spectrum, drift-force coefficient and wave spectrum as functions of angular frequency

7.6.7 Wave Drift Damping

In forward speed and in coastal currents the slowly varying motion may be damped by the fact that the encountered wave period and subsequently the wave drift coefficient varies during the slow surge causing a kind of hysteretic damping, called wave-drift damping. As we have negligibly small slowly varying motion in the present case, it is not useful to take this into account.

7.6.8 Combined Maximum Excursions

Using the design format according to Sect. 7.5.1.1 we end up with the following table over the design motions X_{C1} and X_{C2} (Table 7.17).

Table 7.17 Design offsets for quasi-static design

Mean offset	Stiffness							
Wave-frequency amplitude								Low-frequency amplitude
Design offset								Lifted chain length at X_{C2}
(m)	(kN/m)	(m)		(m)		(m)		(m)
		Sign.	Max.	Sign.	Max.	X_{C1}	X_{C2}	
2.6	12	5.2	9.7	0	0	7.8	12.3	424

Diffraction results with equivalent drag damping

The calculation shows that if we use the tangent stiffness modulus (12 kN/m) of the mooring system we fulfil the lifting criterion that the up-wave chain should rest on the bottom close to the anchor. However, in Sect. 7.5.1.2.1 it is shown that we do not fulfil the tension criterion, why a second design loop was performed.

7.7 Conclusions

The following conclusions can be drawn from the design exercise

- Simplified drag and wind coefficients can be used, because the mean offset is not a dominant part of the total horizontal displacement.
- The Morison wave formulation can be used for objects smaller than 1/4th of the wavelength, however with some overdesign. It is important to test various wave frequencies and realistic wave amplitudes. Used in the frequency-domain equivalent linearized drag damping must be added to compensate for the dropped drag term.
- Using the diffraction method for small objects, equivalent linearized drag damping must be added.
- In the equation of motion, there is a difficulty with progressively stiffening moorings. In the CALM system choosing a stiffness around the mean offset will not give a realistic motion as the stiffness may vary one order of magnitude during the oscillation. It is advised to use time-domain simulations taking at least $S(x)$ into consideration, and then the drag damping could as well be introduced as $b(\dot{x}) = CA\,1/2\,\rho|\dot{x}|$.
- In a final design, time-domain design tools including mooring dynamics should be used complemented by large-scale model tests.
- Other types of moorings as e.g. synthetic fibre ropes in taut configuration or with buoys and lump weights may better fulfil demands on footprint and non-resonant motions. The weight of the chains may cause a large vertical force on the floater, which may constitute a problem. For taught systems the anchoring must take vertical lifting forces, which must be studied.

Acknowledgments The underlying study was carried out at Dept. of Shipping and Marine Technology, Chalmers, and was co-funded from Region Västra Götaland, Sweden, through the Ocean Energy Centre hosted by Chalmers University of Technology, and the Danish Council for Strategic Research under the Programme Commission on Sustainable Energy and Environment (Contract 09-067257, Structural Design of Wave Energy Devices).

References

1. Bergdahl, L., McCullen, P.: Development of a Safety Standard forWave Power Conversion Systems. Wave Energy Network, CONTRACT N°: ERK5 - CT - 1999-2001 (2002)
2. Bergdahl, L., Mårtensson, N.: Certification of wave-energy plants—discussion of existing guidelines, especially for mooring design. In: Proceedings of the 2nd European Wave Power Conference, pp. 114–118. Lisbon, Portugal (1995)
3. Johanning, L., Smith, G.H., Wolfram, J.: Towards design standards for WEC moorings. In: Proceedings of the 6th Wave and Tidal Energy Conference, Glasgow, Scotland (2005)
4. Paredes, G., Bergdahl, L., Palm, J., Eskilsson, C., Pinto, F.: Station keeping design for floating wave energy devices compared to floating offshore oil and gas platforms. In: Proceedings of the 10th European Wave and Tidal Energy Conference 2013
5. Position Mooring, DNV Offshore Standard DNV-OS-E301, 2013
6. Guidelines on design and operation of wave energy converters, Det Norske Veritas, 2005 (Carbon Trust Guidelines)
7. SWAN, Simulating Waves Nearshore. http://swanmodel.sourceforge.net/. Accessed 10 Aug 2015
8. http://www.mikepoweredbydhi.com/-/media/shared%20content/mike%20by%20dhi/flyers%20and%20pdf/product-documentation/short%20descriptions/mike21_sw_fm_short_description.pdf. Accessed 19 Aug 2015
9. Recommended Practice DNV-RP-C205, October 2013
10. Long-term Wave Prediction, Structural Design of Wave Energy Devices, Deliverable D1.1, DHI, Erwan Tacher, Jacob V Tornfeldt Sørensen, Maziar Golestani, 10 April 2013
11. Pecher, A., Kofoed, J.P.: Experimental study on the structural and mooring loads of the WEPTOS Wave Energy Converter. Aalborg: Department of Civil Engineering, Aalborg University. (DCE Contract Reports; No. 142) (2014)
12. Sterndorf, M.: WavePlane, Conceptual mooring system design, Sterndorf Engineering, 15 November 2009
13. Margheritini, L.: Review on available information on wind, water level, current, geology and bathymetry in the DanWEC area, (DanWEC Vaekstforum 2011), Dep. Civil Engineering, Aalborg University, Aalborg, DCE Technical Report, No 135 (2012)
14. Pecher, A., Foglia, A., Kofoed, J.P.: Comparison and sensitivity investigations of a CALM and SALM type mooring system for WECs
15. Faltinsen, O.M.: Sea Loads on Ships and Offshore Structures. Cambridge University Press (1990)
16. Sachs, P.: Wind Forces in Engineering, 2nd edn. Elsevier (1978) ISBN: 978-0-08-021299-9
17. Haddara, M.R., Guedes, C.: Soares: wind loads on marine structures. Marine Struct. **12**, 199–209 (1999)
18. Longuet-Higgins, H.C.: The mean forces exerted by waves on floating or submerged bodies with application to sand bars and wave-power machines. Proc. R. Soc. London **A352**, 462–480 (1977)
19. Maruo, H.: The drift of a body floating on waves. J. Ship Res. **4** (1960)
20. Sesam, DeepC, DNV Softwares. http://www.dnv.com/services/software/products/sesam/sesamdeepc/. Accessed 03 Nov 2013

21. Sarpkaya, T., Isaacson, M.: Mechanics of Wave Forces on Offshore Structures, Van Nostrand Reinhold Company (1981) ISBN 10: 0442254024/ISBN 13: 9780442254025
22. Chakrabarti, S.K.: Handbook of offshore engineering, vol. 1. Elsevier (2005)
23. Yeung, R.: Added mass and damping of a vertical cylinder in finite-depth waters. Appl. Ocean Res. **3**(3), 119–133 (1981) ISSN 0141-1187
24. Johansson, M.: Transient motion of large floating structures, Report Series A:14, Department of Hydraulics, Chalmers University of Technology (1986)
25. Ramsey, A.S.: Statics. The University Press, Cambridge (1960)
26. Selmer, J.: Forankrings- og fortøyningssystemer. Beskrivelse av analysmetodikk og belastningforhold. Course: Kjetting, ståltau og fibertau, Norske sivilingenjørers forening, 1979
27. http://www.sotra.net/products/tables/stength-for-studlink-anchor-chain-cables. Accessed 05 May 2014
28. http://www.sotra.net/products/tables/weight-for-studlink-anchor-chain. Accessed 22 May 2014
29. Bergdahl, L.M., Rask, I.: Dynamic vs. Quasi-Static Design of Catenary Mooring System, 1987 Offshore Technology Conference, OTC 5530
30. Muliawan, M.J., Gao, Z., Moan, T.: Analysis of a two-body floating wave energy converter with particular focus on the effect of power take off and mooring systems on energy capture. In: OMAE 2011, OMAE2011-49135
31. Sesam, MIMOSA, DNV Softwares. http://www.dnv.com/services/software/products/sesam/sesamdeepc/mimosa.asp. Accessed 03 Nov 2013
32. Orcaflex Documentation. http://www.orcina.com/SoftwareProducts/OrcaFlex/Documentation/OrcaFlex.pdf. Accessed 03 Nov 2013
33. ZENMOOR Mooring Analysis Software for Floating Vessels. http://www.zentech-usa.com/zentech/pdf/zenmoor.pdf. Accessed 03 Dec 2012
34. Sesam SIMO, DNV Softwares. http://www.dnv.com/services/software/products/sesam/sesamdeepc/simo.asp. Accessed 03 Nov 2013
35. Parmeggiano, S. et al.: Comparison of mooring loads in survivability mode of the wave dragon wave energy converter obtained by a numerical model and experimental data. In: OMAE 2012, OMAE2012-83415
36. CASH, In-house program, GVA. http://www.gvac.se/engineering-tools/. Accessed 03 Nov 2013
37. Thunder Horse Production and Drilling Unit. http://www.gvac.se/thunder-horse/. Accessed 03 Nov 2013
38. Gao, Z., Moan, T.: Mooring system analysis of multiple wave energy converters in a farm configuration. In: Proceedings of the 8th European Wave and Tidal Energy Conference, Uppsala, Sweden (2009)
39. Pizer, D.J. et al.: Pelamis WEC—Recent advances in the numerical and experimental modelling programme. In: Proceedings of the 6th European Wave and Tidal Energy Conference, Glasgow, UK (2005)
40. Ma, Q.W., Yan, S.: QALE-FEM for numerical modelling of nonlinear interaction between 3D moored floating bodies and steep waves. Int. J. Numer. Meth. Engng. **78**, 713–756 (2009)
41. Palm, J. et al.: Coupled mooring analysis for floating wave energy converters using CFD: Formulation and validation. Int. J. Mar Energy (May 2016). doi: 10.1016/j.ijome.2016.05.003
42. Yu, Y., Li, Y.: Preliminary result of a RANS simulation for a floating point absorber wave energy system under extreme wave conditions. In: 30th International Conference on Ocean, Offshore, and Arctic Engineering, Rotterdam, The Netherlands, 19–24 June 2011
43. Jack/St Malo Deepwater Oil Project. http://www.offshore-technology.com/projects/jackstmalodeepwaterp/. Accessed 03 Nov 2013
44. Jack & St Malo Project, Response-based analysis, GVA, KBR, Göteborg, 2010, Internal report
45. Craig Roy, Jr. R.: Structural Dynamics. Wiley, New York (1981)

46. Roberts, J.B., Spanos, P.D.: Random vibration and statistical linearization. Wiley, Chichester (1990)
47. William, T.: Thompson: Theory of Vibration with Applications. Prentice-Hall Inc., Englewood Cliffs (1972)
48. Pinkster, J.A.: Low-frequency phenomena associated with vessels moored at sea. Soc. Petrol. Eng. J. pp. 487–494 (1975)
49. Newman, J.N.: Second Order Slowly Varying Forces on Vessels in Irregular Waves. In: Bishop, R.E.D, Price, W.G. (eds.) Proceedings of International Symposium Dynamics of Marine Vehicles and Structures in Waves. pp. 182–186. London Mechanical Engineering Publications LTD (1974)